

Cenozoic evolution of eastern Iberia: Structural data and dynamic model

JOAN GUIMERÀ

Grup de Geodinàmica i Anàlisi de Conques. Departament de Geologia Dinàmica, Geofísica i Paleontologia. Universitat de Barcelona.
Martí i Franqués s/n. E-08071 Barcelona. e-mail: joang@natura.geo.ub.es

RESUM

Evolució cenozoica d'Ibèria oriental: Dades estructurals i model dinàmic

L'interior d'Ibèria va experimentar diversos episodis de deformació intraplaca durant el Mesozoic i el Cenozoic. La part oriental, durant el Paleogen i el Miocè inferior, va ser sotmesa a compressió i s'hi formà la Cadena Ibèrica (que inclou, també, la Cadena Costanera Catalana); com a resultat van formar-se sistemes d'encavalcaments (orientats NW-SE i E-W) i falles direccionals convergents (NE-SW sinistres i NW-SE dextres). A partir del Miocè inferior, es produí una extensió a les àrees costaneres orientals d'Ibèria i al solc de València, relacionada amb l'obertura de la Mediterrània occidental, que donà lloc a les fosses costaneres de la part oriental d'Ibèria; aquestes fosses van ser determinades per falles normals orientades al voltant de la direcció NE-SW. No obstant això, durant el Miocè inferior les parts més occidentals de la Cadena Ibèrica van restar sotmeses encara a compressió (falles direccionals NW-SE i encavalcaments E-W), quan l'extensió ja havia començat a les parts orientals de la Cadena.

A partir de les dades conegudes sobre la cinemàtica de les falles majors, compresives i extensives, es presenta un model dinàmic simple de l'evolució de la regió, fent servir la fórmula de Bott (1959). Els resultats mostren que tant la compressió com l'extensió poden explicar-se assumint un eix principal d'esforç horitzontal màxim orientat apro-

ximadament N-S, en una direcció similar a la direcció de convergència entre Europa, Ibèria i Àfrica durant el Cenozoic.

Mots clau: Anàlisi de l'esforç. Deformació intraplaca. Encavalcament. Falla direccional. Falla extensiva. Cenozoic. Ibèria. Mediterrània occidental.

ABSTRACT

Iberia underwent intraplate deformation during the Mesozoic and Cenozoic. In eastern Iberia, compression took place during the Palaeogene and early Miocene, giving rise to the Iberian Chain, and extension started during the early Miocene in the coastal areas and the Valencia trough; during early Miocene compression continued in the western Iberian Chain whereas extension had started in the eastern Iberian Chain. From the kinematic data obtained from the major compressional and extensional structures formed during the Cenozoic, a simple dynamic model using Bott's (1959) formula is presented. The results show that both extension and compression may have been produced assuming a main horizontal stress-axis approximately N-S, in a similar direction that the convergence between Europe, Iberia and Africa during the Cenozoic.

Keywords: Stress analysis. Intraplate deformation. Thrust. Strike-slip fault. Extensional fault. Cenozoic. Iberia. Western Mediterranean.

INTRODUCTION

Successive deformations in intraplate areas often produce the reactivation of previous faults which undergo successive motions over time; as a result, inversion tectonics takes place. These successive deformations are the result of changes in the dynamics of the tectonic processes affecting these areas from the plate boundaries, these changes being sharp or progressive. The aim of this paper is to synthetise the evolution of the Iberian Chain and the Catalan Coastal Chain during the Alpine compression and the Neogene extension through time and space and, from the kinematic data collected or deduced in the major faults herein, to propose a dynamic evolution for this area.

GEOLOGICAL SETTING

Palaeogene and Neogene compressional structures:

In the eastern Iberian Peninsula four structural units developed during the Alpine compression, from N to S: the Pyrenees, the Ebro Basin, the Iberian Chain and the Betic Cordillera.

The Pyrenees are the result of the collision between Iberia and the European plate, the convergence occurring from Campanian to Early Miocene. A fold-and-thrust belt involving both the Hercynian basement and the Mesozoic and Cenozoic cover developed as a consequence of this, thrusting on the Ebro basin to the S and on the Aquitain basin to the N. The minimum shortening estimated from a crustal balanced cross-section is 147 km (Muñoz, 1992).

The Ebro Basin formed during the Alpine orogeny as a foreland basin of the Pyrenees to the N and the Iberian Chain to the S. The overall structure of the basin is simple, the Tertiary beds being nearly horizontal over most of their extent and significantly deformed only along the margin of the basin (Anadón, *et al.*, 1985). Its sedimentary fill consists of a thick pile of Tertiary rocks (mainly conglomerates, sandstones, shales and evaporites) which range in age from Palaeocene to Miocene and reach up to 5000 m in thickness (Riba *et al.*, 1983).

In the Iberian Chain all the Alpine deformed areas within the Iberian small-plate have been included (Guimerà *et al.*, 1992): the Catalan Coastal Chain, and the Iberian Chain s.s. NW-SE-, E-W- and NE-SW-oriented compressional Tertiary structures are present within

this chain. Most of them are interpreted to be normal Mesozoic faults which bounded the Mesozoic basins and were inverted during the Palaeogene. Their kinematics depended on the orientation of the faults with respect to the regional compression. Three main units can be distinguished, where structures of different orientations dominate (Guimerà, 1984; Guimerà and Álvaro, 1990):

1. The Catalan Coastal Chain, which is composed of Hercynian basement unconformably overlain by a sedimentary cover of Triassic to Cretaceous age, which is mainly made up of carbonate sequences. The dominant structures are major basement thrusts and faults whose directions range from N 70 E to N 30 E; these faults have a right-stepping, *en échelon* array. During the Paleogene along these NE-SW faults sinistral-convergent wrenching (transpressional) took place, giving rise to monoclines and to basement slices which thrusted on the Mesozoic cover and the Paleogene rocks of the Ebro Basin; evidence for this sinistral movement is provided by (1) horizontal striations on major fault planes within the Mesozoic cover, (2) structures in fault gouges developed in fault planes, (3) *en echelon* folts in the sedimentary cover over basement faults and (4) the change of strike of the low-angle thrusts of the Linking Zone (see below) (Anadón *et al.*, 1985; Guimerà, 1988). Deformation started in the early-middle Eocene and continued, at least, until late Oligocene. There are no younger sedimentary rocks left in contact with the Catalan Coastal Chain structures (Anadón *et al.*, 1985).
2. The Iberian Chain s.s. has a Hercynian basement and a Mesozoic cover similar to that of the Catalan Coastal Chain. Major NW-SE faults affect the basement, often separating folds of a great radius of curvature; these faults are often deformed or inverted normal Mesozoic faults; in the latter case they have a clear reversal component. In several faults, a dextral component in the fault motion is also deduced from (1) striations on some major fault planes in the Mesozoic cover (Guimerà, 1988) and (2) structures in fault gouges in basement faults associated with basement slices showing transpressional deformation (Colomer & Santanach, 1988). Folds and thrusts striking NW-SE form imbricate-thrust systems developed in the Mesozoic cover; they have a double sense of displacement, to the NE and to the SW in the northeast and southwest parts of the chain, respectively. N-S and E-W thrust and fold systems also exist in the basement and the cover. The starting time of deformation is uncertain; late Eocene deformations have been recognized, which continued to upper-

most Oligocene or lower Miocene (Pérez, 1989; González, 1989; Muñoz, 1992); the latest deformations took place in E-W thrusts and NW-SE dextral basement faults (Guimerà, 1984).

3. The Linking Zone is a triangular-shaped area located at the place where the NE-SW and NW-SE structures of the Catalan Coastal Range and the Iberian Range join. It is composed of mainly carbonatic Mesozoic cover, whose thickness reaches 5500 m.; no Hercynian basement crops out. There is an array of E-W trending, N-vergent, low-angle thrusts and folds in its north front that thrusted on the Iberian Chain, Ebro Basin and Catalan Coastal Chain; the slip of these thrusts ranges from 1 to 10 km. Changes of strike in the low-angle thrusts from E-W to near NE-SW show the action of the NE-SW sinistral basement faults of the Catalan Coastal Chain. Deformation took place from, at least, late Eocene to late Oligocene or early Miocene (González, 1989).

The age of formation of the structures of the former units show their contemporaneity, at least during late Eocene and Oligocene times; uncertainty of the beginning of deformation in the Iberian Chain and the Linking Zone does not allow us to assert that this synchrony of deformation was also produced during early-middle Eocene). Geometrical relationships between structures of the three units also show a synchrony in their development: (1) change of strike of the low-angle thrusts of the Linking Zone over NE-SW basement faults of the Catalan Coastal Chain may be explained by the contemporary sinistral component of these faults; (2) interference between E-W and NW-SE structures of the Linking Zone and the Iberian Chain show two different geometrical relationships: (a) NW-SE structures developed before the E-W ones (Simón Gómez, 1980) and (b) both directions of structures developed simultaneously (Guimerà, 1988).

Neogene extensional structures: the Catalan-Valencian domain

From lower Miocene or uppermost Oligocene, extension took place in the eastern part of the area studied. NE-SW to N-S and NW-SE major basement faults became normal faults, giving rise to the formation of a widespread horst and graben system overprinted on the compressional former units. The area affected by this extension spreads both in the emerged eastern Iberia coastal areas and offshore from them, constituting the Catalan-Valencian domain (Fontboté *et al.*, 1990).

The western boundary of the extensional area related to the Catalan-Valencian domain is defined in the northern parts of the domain by an array of NE-SW faults, near the coast, displaying an *én échelon* arrangement inherited from the compressional structures: the Vallès-Penedès, El Camp and Baix Ebre faults, whereas in the southern areas this boundary is less defined, around the faults that limit the Teruel graben, farther to the W. The tectonic inversion was very dramatic in some cases: the N 70 E Vallès-Penedès fault (NW of Barcelona) had a sinistral-convergent slip, producing plurikilometric basement monoclines and slices with more than 4 km of horizontal slip during Paleogene whereas it had a 3 km normal slip from lower Miocene.

Extension probably started during the latest Oligocene or Early Miocene (Soler *et al.*, 1983; Bartrina *et al.*, 1992) and two main stages can be distinguished: 1) a synrift stage of late Oligocene-Burdigalian age, and 2) a postrift stage, which last up to the present (Díaz del Río *et al.*, 1986, Roca *et al.*, 1990; Bartrina *et al.*, 1992). During the early Miocene, when coastal rifts developed, contractional deformation continued in the central and western Iberian Chain, as shown by 1) the dextral slip still in the NW-SE in the Daroca fault basement fault (Colomer and Santanach, 1988) west of the Teruel graben and 2) the continuation of the motion of the E-W-striking N-directed Cameros thrust (Guimerà and Álvaro, 1990; Casas Sáinz, 1992, 1993). Extension did not reach those western areas until the Pliocene, when the Jiloca graben was formed (Simón-Gómez, 1989).

After Roca and Guimerà (1992) the extension in the Catalan-Valencian domain was accommodated by a normal fault system detached at 13-15 km depth, following a simple shear model in the upper crust. Taking into account that the main Neogene normal faults involving the basement are inherited at least from the Paleogene compression (and, most of them, perhaps from Mesozoic times: Salas, 1987; Roca and Guimerà, 1992) and that the proposed thin-skinned thrust model for the Iberian Chain during Palaeogene times assumes a detachment level at the western areas of about 7-11 km depth (Guimerà and Álvaro, 1990), the possibility arises that the same overall system of faults, having the same basal detachment, underwent contraction during the Palaeogene and extension during the Neogene. This has been proposed (Roca, 1992) for the coastal areas, where clearly the Palaeogene contractional faults of the Catalan Coastal Chain were inverted producing the Neogene grabens, but it may be extended to the whole area studied.

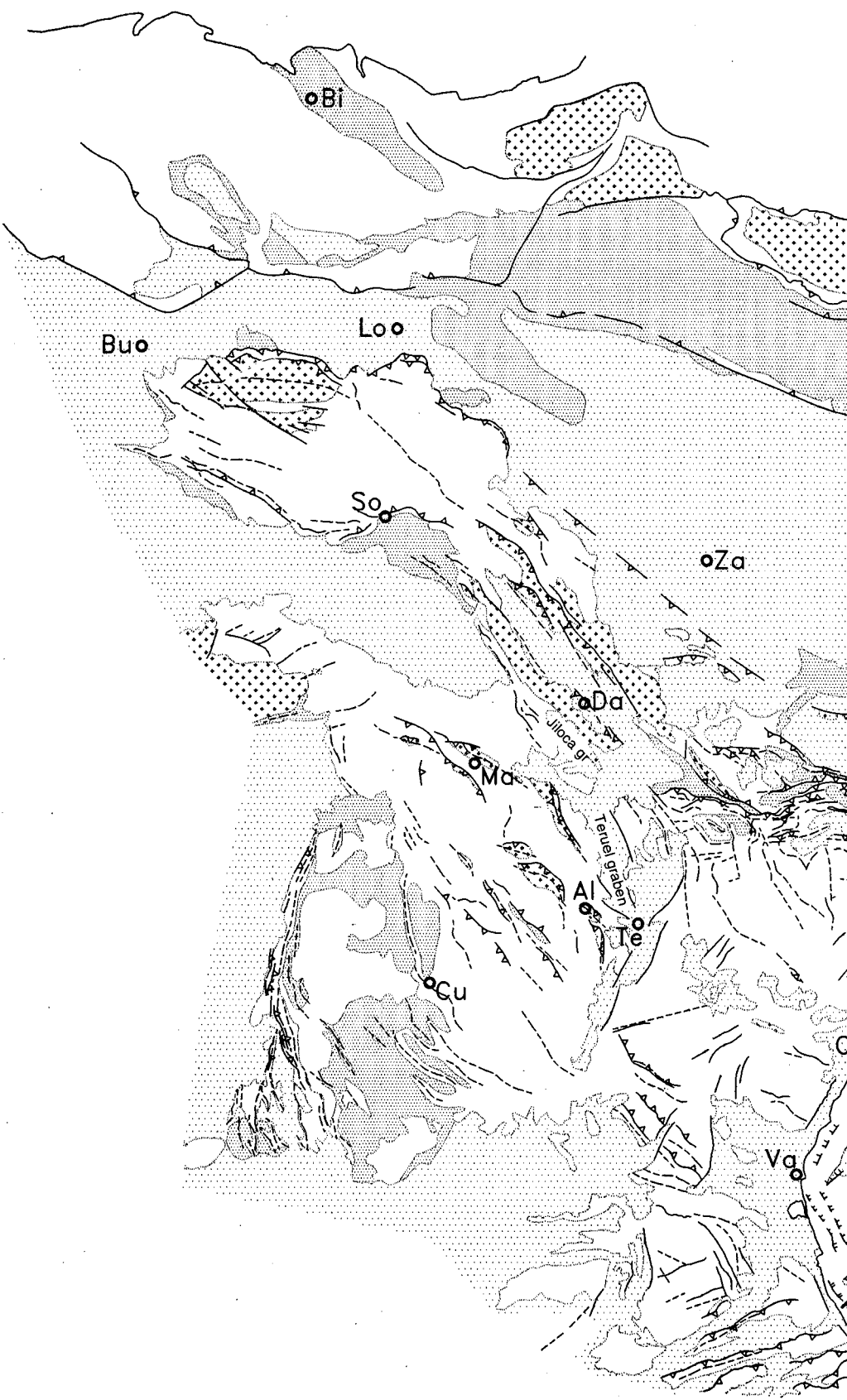


Figure 1: Structural map of the eastern Iberia and the western Valencia trough. Data from Fontboté et al. (1974), Guimerà and Álvaro (1990) for the Iberian Chain, Roca (1992) for the Valencia trough and Vergés (1993) for the Pyrenees. In the offshore, only the rocks filling the main Lower Miocene grabens are shown.

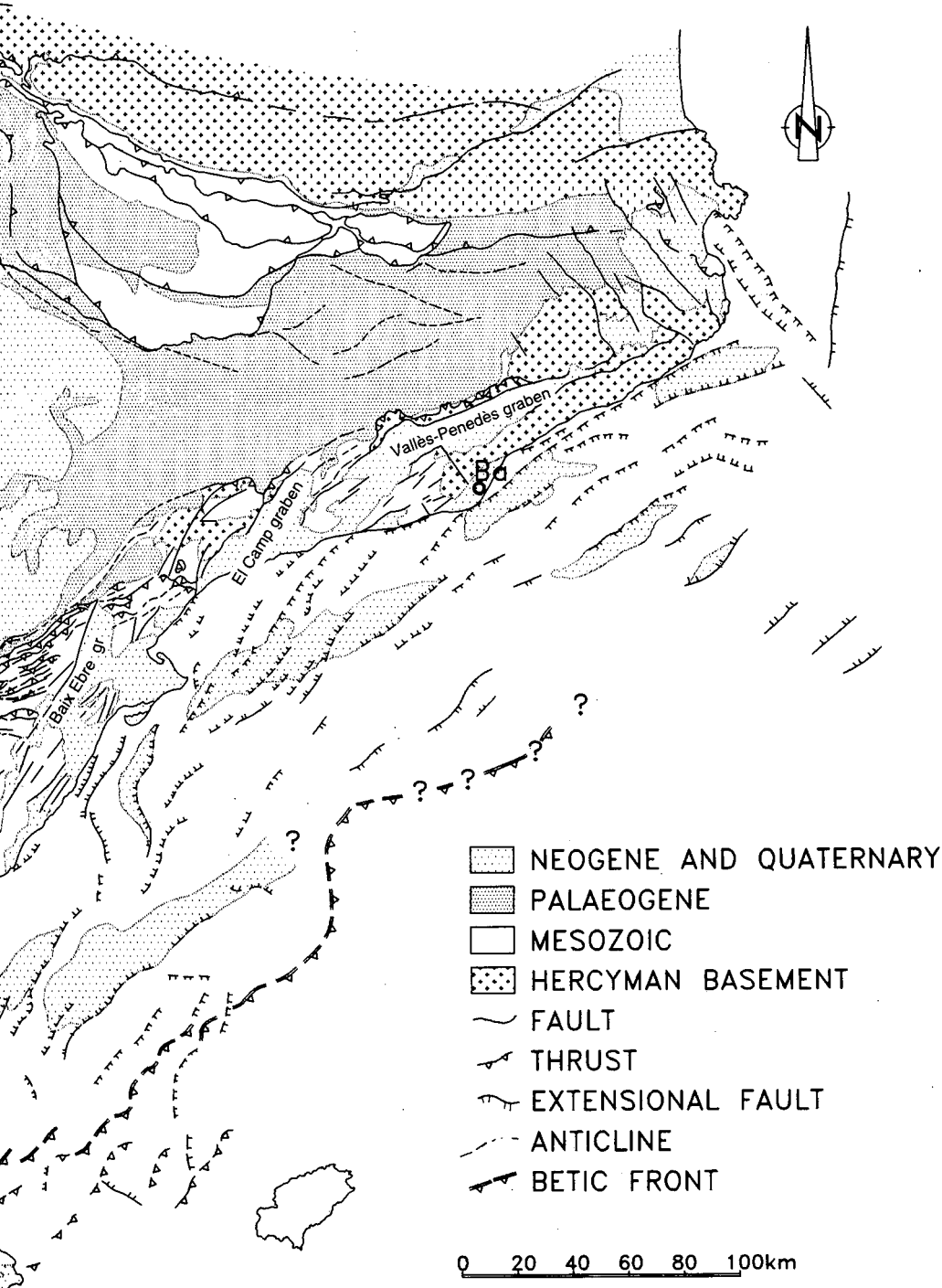


Figura 1: Mapa estructural de la part oriental d'Ibèria i del solc de València. Fet amb dades de Fontboté et al. (1974), Guimerà i Álvaro (1990) per la Cadena Ibèrica, Roca (1992) pel solc de València i Vergés (1993) pels Pirineus. A les regions submergides, només es mostren els gràbens principals d'edat miocena inferior.

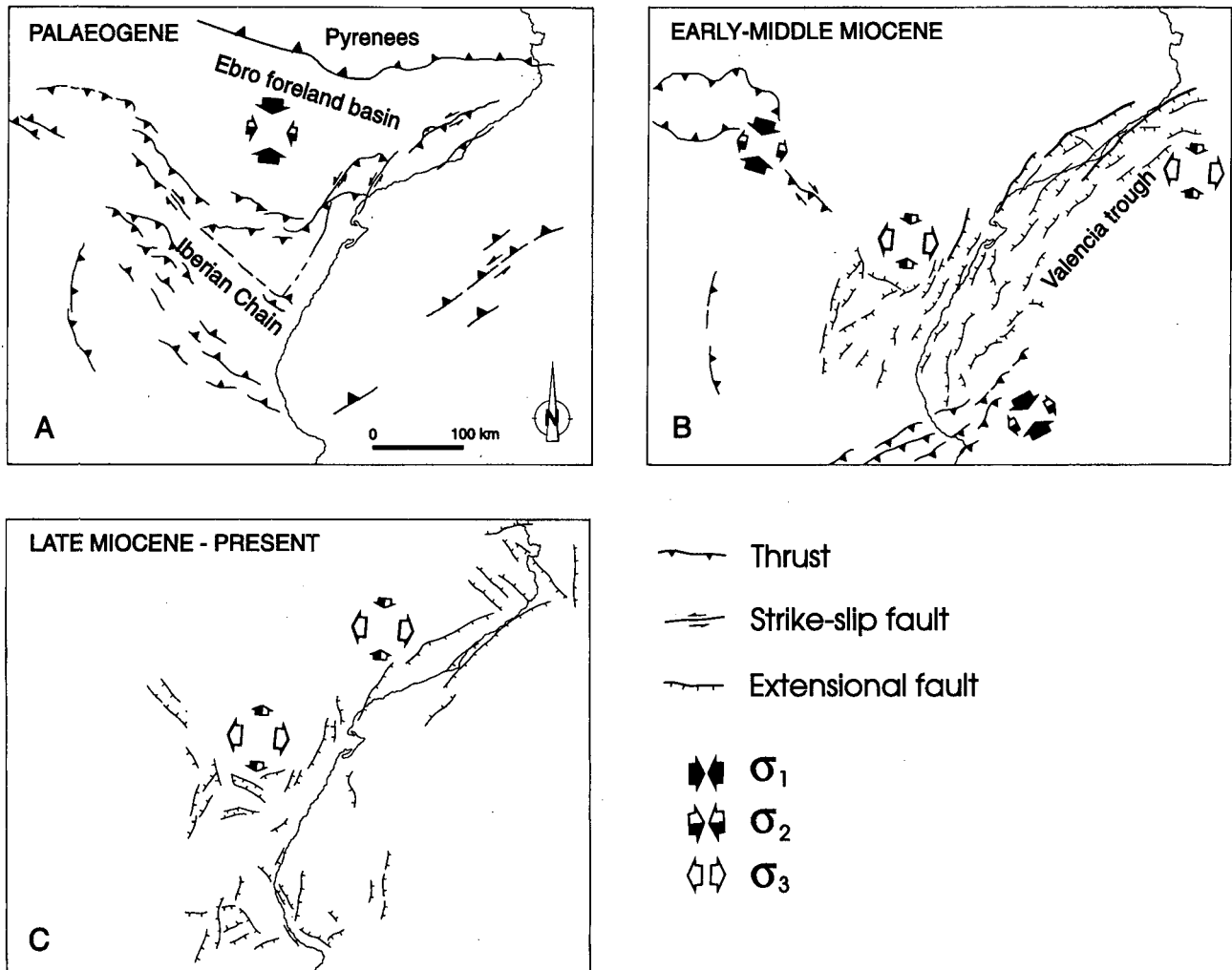


Figure 2: Cenozoic evolution of the Iberian Chain and western Valencia trough. The tectonic sketch is based in Guimerà (1988) and Guimerà and Roca (*in Guimerà et al.*, 1992, fig. 102). Centripetal arrows mean compression; centrifugal arrows mean tension.

Figura 2: Evolució cenozoica de la Cadena Ibèrica i de la part oriental del solc de València. L'esquema tectònic està fet a partir de Guimerà (1988) i Guimerà i Roca (*in Guimerà et al.*, 1992, fig. 102). Quan les fletxes són centrípetes indiquen compressió, quan són centrífugues indiquen tensió.

DYNAMIC MODEL

From the above, the migration of the beginning of the compression from N to S and of the end of the compression from E to W may be deduced; the latter producing the coexistence, during the early Miocene, of extension in the Catalan-Valencian domain and compression in the western areas of the Iberian Chain.

A summary of the fault motions in the region studied shows that, in the compressional structures, thrusting motions took place on the approximatively E-W faults within the Iberian Chain (the Linking Zone and the Cameros unit) and the Pyrenees, whereas sinistral strike-slip com-

ponents are deduced from the NE-SW basement faults of the Catalan Coastal Chain and dextral ones from some NW-SE basement faults in the Iberian Chain, the convergent component on these faults being clearly observed in the ENE-WSW faults of the Catalan Coastal Chain and being the dominant one in the NW-SE faults of the Iberian Chain. The extensional structures (mostly NE-SW to N-S) have a dominant dip-slip normal motion, but some sinistral component has been observed on some NE-SW faults in the Penedès area Bartrina *et al.* (1992).

In order to calculate the movement on the different fault planes described above under different stress-fields,

the formula of Bott (1959) has been used. This formula is:

$$\tan \theta = \frac{n}{lm} \left[m^2 - (1-n^2) \frac{\sigma_z - \sigma_x}{\sigma_y - \sigma_x} \right]$$

where θ is the pitch of the slip on the fault plane, σ_y is the horizontal major stress-axis, σ_x is the horizontal minor stress-axis, σ_z is the vertical stress-axis and l, m and n the direction cosines of the fault plane with respect to the main stress-axes.

Assuming $\sigma_y \geq \sigma_x$ and taking into account the axial relation

$$R_B = \frac{\sigma_z - \sigma_x}{\sigma_y - \sigma_x}$$

R_B varies from $-\infty$ to $+\infty$. The value of R_B indicates the shape of the stress ellipsoid and the spatial position of σ_1 , σ_2 and σ_3 (Armijo, 1977), according to the following table:

	horizontal axes $\sigma_2 \sigma_3$	vertical axis σ_1
$R_B > 1$	$\sigma_1 \sigma_3$	σ_2
$0 < R_B < 1$	$\sigma_1 \sigma_2$	σ_3
$R_B < 1$		

there are two particular cases:

$R_B = 1$, where σ_3 is horizontal and $\sigma_1 = \sigma_2$ and

$R_B = 0$, where σ_1 is horizontal and $\sigma_2 = \sigma_3$.

Differently oriented fault planes have been chosen to model the major fault recognized in the study region (Table 1). The chosen values of the axial relation R_B constitute a span of the possible stress ellipsoids:

$R_B = 1$: σ_3 is vertical and $\sigma_1 > \sigma_2$. There is compression in the direction of σ_1

$R_B = 0$: σ_1 is horizontal and $\sigma_2 = \sigma_3$.

$R_B = 0.3$: σ_2 is vertical and the three main stress-axes have different relative values.

$R_B = 1$: σ_3 is horizontal and $\sigma_1 = \sigma_2$.

$R_B = 3$: σ_1 is vertical and the three main stress-axes have different relative values. There is a dominant extension parallel to σ_3 .

$R_B = 8$: σ_1 is vertical and the values of σ_2 and σ_3 are close. There is a horizontal extension in all directions.

Taking into account the dextral-slip component deduced in some NW-SE faults in the Iberian Chain and the general sinistral-slip component in the ENE-WSW to NNE-SSW faults in the Catalan Coastal Chain, an approximately N-S compression direction is deduced from these structures during the Palaeogene (Guimerà, 1983, 1984; Guimerà and Álvaro, 1990) and, from the ENE-WSW to N-S normal faults bounding the rifts of the Catalan-Valecian domain, an overall E-W extension direction may be deduced during the Neogene (Guimerà, 1983, 1984; Fontboté *et al.*, 1990; Roca, 1992). Calculations have been performed supposing σ_y at different orientations around the N-S direction. The results that best fit the kinematics of the structures described above are obtained when $\sigma_y = N010E$ and $N020E$ (Table 1).

DISCUSSION

I shall focus first on the R_B values implying $\sigma_y = \sigma_1$ ($-10 \leq R_B < 1$) and the faults striking N135E (Iberian Chain), N075E (northern Catalan Coastal Chain) and N030E (southern Catalan Coastal Chain, coastal Linking Zone and Iberian Chain). In the N135E faults, reverse-dextral to dextral motions are obtained depending on the R_B value and the fault-plane dip; similar results are obtained in the N075E faults, the motion being, in that case, reverse-sinistral to sinistral, whereas in the N030E faults, purer sinistral motions are obtained (Table 1).

In the case of the N135E and N075E faults, the angle which they form with the $\sigma_y = \sigma_1$ direction is 55° to 65° , that is, a much higher angle than the optimum 30° ; which implies a significant compression perpendicular to these faults. Transpressional deformation has been related to both types of fault; in the Iberian Chain, where the NW-SE thrusts dominate over the parallel strike-slip dextral faults, a decoupling of the oblique convergence producing horizontal motions on the strike-slip faults and dip-slip motions on the thrusts has been proposed (Guimerà & Álvaro, 1990), similarly to what has been proposed in diverse geological contexts by Fitch (1972), Eisbacher (1985), Beck (1986) and Mount and Suppe (1987).

FAULT								
$\sigma_y = N-S$	$R_B = -10$	$R_B = -1$	$R_B = 0$	$R_B = 0.3$	$R_B = 1$	$R_B = 3$	$R_B = 8$	
1 135 60 SW	81 SE id	43 SE di	17 SE di	7 SE di	17 NW dn	57 NW nd	78 NW nd	
2 135 80 SW	69 SE id	20 SE di	7 SE di	3 SE di	7 NW dn	31 NW dn	61 NW nd	
3 155 60 SW	78 SE id	29 SE di	5 SE di	3 NW dn	21 NW dn	53 NW nd	75 NW nd	
4 155 80 SW	62 SE id	13 SE di	2 SE di	1 NW dn	9 NW dn	28 NW dn	56 NW nd	
5 175 60 E	77 N id	24 N di	0 d	7 S dn	23 S dn	52 S nd	74 S nd	
6 175 80 E	60 N id	10 N di	0 d	3 S dn	10 S dn	27 S dn	54 S nd	
7 105 80 NE	82 W id	52 W id	32 W di	23 W di	3 E dn	54 E nd	78 E nd	
8 105 85 NE	75 W id	33 W di	17 W di	12 W di	1 E dn	35 E dn	67 E nd	
9 85 60 S	89 W is	84 W is	79 W is	74 W is	2 E sn	84 E ns	88 E ns	
10 85 80 S	87 W is	76 W is	63 W is	54 W is	1 E sn	76 E ns	86 E ns	
11 85 85 S	85 W is	63 W is	45 W is	35 W si	0 s	63 E ns	82 E ns	
12 75 60 SE	87 W is	73 W is	57 W is	47 W is	6 E sn	74 E ns	85 E ns	
13 75 80 SE	82 W is	52 W is	32 W si	23 W si	3 E sn	54 E ns	78 E ns	
14 50 60 SE	82 W is	47 W is	22 W si	11 W si	16 E sn	58 E ns	79 E ns	
15 50 80 SE	70 W is	23 W si	9 W si	4 W si	6 E sn	33 E sn	63 E ns	
16 30 60 SE	79 W is	32 W si	7 W si	1 E sn	21 E sn	54 E ns	76 E ns	
17 30 80 SE	64 W is	14 W si	3 W si	1 E sn	8 E sn	29 E sn	57 E ns	
$\sigma_y = N010E$								
1 135 60 SW	83 SE id	52 SE id	27 SE di	16 SE di	14 NW dn	60 NW nd	80 NW nd	
2 135 80 SW	73 SE id	26 SE di	11 SE di	6 SE di	6 NW dn	35 NW dn	65 NW nd	
3 155 60 SW	80 SE id	35 SE di	10 SE di	1 SE di	20 NW dn	55 NW nd	76 NW nd	
4 155 80 SW	65 SE id	16 SE di	4 SE di	0 d	8 NW dn	29 NW dn	58 NW nd	
5 175 60 E	78 N id	26 N di	2 N di	6 S dn	23 S dn	53 S nd	74 S nd	
6 175 80 E	61 N id	11 N di	1 N di	2 S dn	9 S dn	27 S dn	55 S nd	
7 105 80 NE	87 W id	76 W id	63 W id	54 W id	1 E dn	76 E nd	86 E nd	
8 105 85 NE	85 W id	63 W id	45 W id	35 W di	0 d	63 E nd	82 E nd	
8bis 105 30 N		89 W id	84 E id	79 W id	74 W id	2 E d	84 E nd	88 E nd
9 85 60 S	87 W is	73 W is	57 W is	47 W is	6 E sn	74 E ns	85 E ns	
10 85 80 S	82 W is	52 W is	32 W si	23 W si	3 E sn	54 E ns	78 E ns	
10bis 85 30 S		87 W is	73 W is	57 W si	47 W is	6 E sn	74 E ns	85 E ns
11 85 85 S	75 W is	33 W si	17 W si	12 W si	1 E sn	35 E sn	67 E ns	
12 75 60 SE	85 W is	62 W is	40 W si	28 W si	10 E sn	66 E ns	82 E ns	
13 75 80 SE	77 W is	36 W si	18 W si	12 W si	4 E sn	41 E sn	71 E ns	
18 75 85 SE	66 W is	21 W si	10 W si	6 W si	2 E sn	24 E sn	56 E ns	
14 50 60 SE	80 W is	39 W si	13 W si	4 W si	18 E sn	56 E ns	77 E ns	
15 50 80 SE	67 W is	18 W si	5 W si	1 W si	7 E sn	30 E sn	59 E ns	
16 30 60 SE	78 W is	27 W si	3 W si	5 E sn	22 E sn	53 E ns	75 E ns	
17 30 80 SE	61 W is	11 W si	1 W si	2 E sn	9 E sn	28 E sn	55 E ns	
$\sigma_y = N020E$								
1 135 60 SW	85 SE id	62 SE id	40 SE di	28 SE di	10 NW dn	66 NW nd	82 NW nd	
2 135 80 SW	77 SE id	36 SE di	18 SE di	12 SE di	4 NW dn	41 NW dn	71 NW nd	
3 155 60 SW	81 SE id	43 SE di	17 SE di	7 SE di	17 NW dn	57 NW nd	78 NW nd	
4 155 80 SW	69 SE id	20 SE di	7 SE di	3 SE di	7 NW dn	31 NW dn	61 NW nd	
5 175 60 E	78 N id	29 N di	5 N di	3 S dn	21 S dn	53 S nd	75 S nd	
6 175 80 E	62 N id	13 N di	2 N di	1 S dn	9 S dn	28 S dn	56 S nd	
7 105 80 NE	87 E is	76 E is	63 E is	54 E is	1 W sn	76 W ns	86 W ns	
8 105 85 NE	85 E is	63 E is	45 E is	35 E si	0 s	63 W ns	82 W ns	
9 85 60 S	85 W is	62 W is	40 W si	28 W si	10 E sn	66 E ns	82 E ns	
10 85 80 S	77 W is	36 W si	18 W si	12 W si	4 E sn	41 E sn	71 E ns	
11 85 85 S	66 W is	21 W si	10 W si	6 W si	2 E sn	24 E sn	56 E ns	
12 75 60 SE	83 W is	52 W is	27 W si	16 W si	14 E sn	60 E ns	80 E ns	
13 75 80 SE	73 W is	26 W si	11 W si	6 W si	6 E sn	35 E sn	65 E ns	
14 50 60 SE	79 W is	32 W si	7 W si	1 E sn	21 E sn	54 E ns	76 E ns	
15 50 80 SE	64 W is	14 W si	3 W si	1 E sn	8 E sn	29 E sn	57 E ns	
16 30 60 SE	77 W is	24 W si	1 W si	7 E sn	23 E sn	53 E ns	74 E ns	
17 30 80 SE	60 W is	10 W si	0 s	3 E sn	10 E sn	27 E sn	54 E ns	

Another explanation for the dominance of the reverse motion on the NW-SE faults in the Iberian Chain is based on the interference of the NW-SE and NE-SW faults around the Linking Zone. During the Neogene extension, the NE-SW faults clearly continued to the SW and cut the NW-SE faults. Assuming the same cutting relation during the Palaeogene, the NE-SW faults might obstruct the strike-slip motion on the NW-SE faults, producing a rising of the stress value parallel to σ_x and, in consequence, a dropping of R_B and an increase in the reverse component of the NW-SE faults.

The faults striking more E-W (N085E to N105E) have a purer dip-slip reverse motion in the model, which is coherent with the approximately E-W thrust systems in the Linking Zone and the Cameros-Demanda unit.

The R_B values implying $\sigma_y = \sigma_2$ ($1 \leq R_B < 8$) and $\sigma_x = \sigma_3$ produce normal-dextral motions on N135E-striking faults and normal-sinistral motions on N075E- to N-030E-striking faults. The last has been observed on some faults in the SE margin on the Vallès-Penedès graben (Guimerà, 1988; Bartrina *et al.*, 1992).

From what has been said up to now, maintaining σ_y oriented N010-020E and changing the R_B values, the kinematics of the major faults in the studied region during both the Palaeogene compression and the Neogene extension may be explained. What is needed is to vary the relative values of the three main stress axes without changing their orientation, obtaining successive coaxial stress fields which changed from stress tensors having $\sigma_y = \sigma_1$ (Palaeogene compressional stage) to stress tensors with $\sigma_y = \sigma_2$ and $\sigma_x = \sigma_3$ (Neogene extensional stage).

Studies carried out on populations of mesostructural faults (Simón Gómez, 1982; Guimerà, 1984, 1988) point to a progressive transition between a horizontal compressive state (which can be correlated to the compressional macrostructures) to an extensional state (correlated to the formation of the extensional macrostructures).

Table 1: Results obtained from applying Bott's (1959) formula to different oriented faults observed –or supposed– in the Iberian Chain assuming three different orientations of the main horizontal stress-axis (σ_y) and different axial relations R_B . In the results obtained using $\sigma_y=N010E$, those which are coherent with the compressional macrostructures are shown in bold and those coherent with the extensional macrostructures are shown in italic. n: normal fault, i: reverse fault, d: dextral fault, s: sinistral fault.

Taula 1: Aplicació de la fórmula de Bott (1959) a falles amb diferents orientacions observades –o suposades– a la Cadena Ibèrica. La taula mostra els resultats obtinguts per tres orientacions diferents de l'eix d'esforç horitzontal principal (σ_y) i diversos valors de la relació axial R_B . Els resultats obtinguts amb $\sigma_y=N010E$, els que són coherents amb les macroestructures compressives són indicats en negreta i els coherents amb les macroestructures extensives es mostren en cursiva. n: falla normal, i: falla inversa, d: falla dextra, s: falla sinistra.

This reinforces the hypothesis proposed in the previous paragraph.

To explain such an evolution of stresses, an attenuation of stresses within Iberia in a N-S direction in time and space has been proposed (Guimerà, 1983 and 1984), as a result of the convergent motion of the European and African plates in a roughly N-S direction, following the model proposed by Tapponnier (1977) and Bousquet and Philip (1981) for the evolution of the west Mediterranean Alpine belt. Variations in the magnitude of stresses produced by this collision could explain the formation and succession of both Paleogene compressional and Neogene extensional major structures, which may have originated within the framework of the same large-scale geotectonic process.

An alternative and, in part, complementary explanation can be drawn taking into account that the main convergence boundary between Africa and Eurasia shifted (after Sristava *et al.*, 1990) from the Pyrenees (where it had been taken place since the mid-Eocene) to the Betic chain (since late Oligocene) at the same time that the opening of the western Mediterranean basin started (also late Oligocene after Biju Duval and Montardet, 1977). This shifting of the main convergence boundary from the Pyrenees to the Betics might result in a dropping of the stress value in the N-S direction within Iberia, at the same time that an E-W extension, related to the opening of the western Mediterranean, were added in the present Catalan-Valencian domain. The combination of both processes, in time and space can, also, explain the Cenozoic evolution of the western Iberia.

ACKNOWLEDGEMENTS

The author thanks Pere Santanach for the critical review of this paper. This paper is a contribution to the project *Evolución de las cuencas intracontinentales del este de Iberia (Cordillera Ibérica) durante la etapa barremiense-albiense de reactivación del rifting ibérico* (DGICYT PB92-0862-C02010). The research needed to do this paper was also partially financed by the *Comissionat per Universitats i Recerca de la Generalitat de Catalunya* (GRQ94-1048).

REFERENCES

- ANADÓN, P., CABRERA, L., GUIMERÀ, J. and SANTANACH, P.F., 1985: Paleogene strike-slip tectonics and sedimentation along the southeastern margin of the Ebro Basin. In: K.T. Biddle & N. Christie-Blick (eds.) *Strike-slip Tect. and Sedim.* Soc. Econ. Paleon. Min. Sp. Publ. 37: 303-318.
- ARMIJO, R., 1977: *La zone de failles de Lorca-Totana (Cordillères Bétiques, Espagne). Etude tectonique et Néotectonique.* Thèse 3ème cycle, Univ. Paris VII, 98 p.
- BECK, M. E., 1986: Model for late Mesozoic-early Tertiary tectonics of coastal California and western Mexico and speculations on the origin of the San Andreas Fault. *Tectonics*, 5(1): 49-64.
- BIJU DUVAL, B. and MONTADERT, L., 1977: Introduction to the structural history of the Mediterranean basins. In: B. Biju Duval and L. Montadert (eds.), *Structural History of the Mediterranean Basins.* Technip, Paris, pp. 1-12.
- BOTT, M.H.P. 1959: The mechanisms of oblique slip faulting. *Geological Magazine*, 96: 109-117.
- BOUSQUET, J.C. and PHILIP, H. 1981: Les caractéristiques de la néotectonique en Méditerranée occidentales. In: F.C. Wezel (ed.): *Sedimentary basins of the Mediterranean margins*, pp. 389-405.
- CASAS SAINZ, A.M., 1992: El frente norte de las Sierras de Cameros: estructuras cabalgantes y campo de esfuerzos. *Zubía*, monográfico, 4, Instituto de Estudios Riojanos, 220 p.
- CASAS SAINZ, A.M., 1993.: Oblique tectonic inversion and basement thrusting in the Cameros Massif (Northern Spain). *Geodinamica Acta*, (Paris) 6(3): 202-216.
- COLOMER, M. and SANTANACH, P., 1988: Estructura y evolución del borde sur-occidental de la Fosa de Calatayud-Daroca. *Geogaceta*, 4: 29-31.
- DIAZ DEL RIO, V., REY, J. and VEGAS, R., 1986. The Gulf of Valencia continental shelf: extensional tectonics in Neogene and Quaternary sediments. *Mar. Geol.*, 73 (1/2): 169-179.
- EISBACHER, G.H., 1985.- Pericollisional strike-slip faults and synorogenic basins, Canadian Cordillera. In: K.T. Biddle & N. Christie-Blick Eds., Sp. Publ.no 37 on *Strike-slip Tectonics and Sedimentation.* Soc. Econ. Paleon. Min., Tulsa, pp. 265-282.
- FITCH, T. J., 1972: Plate Convergence, Transcurrent Faults, and Internal Deformation Adjacent to Southeast Asia and the Western Pacific. *Journal of Geophysical Research*, 77(23): 4432-4460.
- FONTBOTÉ, J.M., GUIMERÀ, J., ROCA, E., SÀBAT, F., SANTANACH, P. and FERNÁNDEZ-ORTIGOSA, F., 1990: The Cenozoic geodynamic evolution of the Valencia trough (western Mediterranean) *Revista de la Sociedad Geológica de España*, 3: 249-259.
- GONZÁLEZ, A., 1989: *Análisis tectosedimentario del terciario del borde SE de la Depresión del Ebro (sector bajoaragones) y de las cubetas ibéricas marginales.* Tesis Univ. Zaragoza. 507 p.
- GUIMERÀ, J., 1983: Évolution de la deformation alpine dans le NE de la Chaîne Ibérique et dans la Chaîne Côtière Catalane. *C. R. Acad. Sc. Paris*, 297: 425-430.
- GUIMERÀ, J., 1984: Paleogene evolution of deformation in the northeastern Iberian Peninsula. *Geological Magazine*, 121: 413-420.
- GUIMERÀ, J., 1988: *Estudi estructural de l'enllaç entre la Serralada ibèrica i la Serralada Costanera Catalana.* PhD. Thesis, Univ. Barcelona, 600 p.
- GUIMERÀ, J., ANADÓN, P., CABRERA, L. et al. 1992: Geología II (Cenozoic). *Història Natural del País Catalans.* vol. 2. Encyclopédia Catalana. 548 p.
- MOUNT, V.S. and SUPPE, J. (1987): State of stress near the San Andreas fault: Implications for wrench tectonics. *Geology*, 15: 1143-1146.
- MUÑOZ, J.A., 1992: Evolution of a continental collision belt: ECORS-Pyrenees crustal balanced cross-section. In: K.R. McClay, ed., *Thrust Tectonics.* Chapman & Hall, pp. 235-246.
- MUÑOZ JIMÉNEZ, A., 1992: *Analisis tectosedimentario del Terciario del sector occidental de la Cuenca del Ebro (Comunidad de La Rioja).* PhD Thesis, Univ. de Zaragoza. Instituto de Estudios Riojanos, 347 p.
- PÉREZ, A., 1989: *Estratigrafía y Sedimentología del Terciario del borde S de la Depresión del Ebro (sector riojano-aragonés) y cubetas de Muniesa y Montalbán.* Tesis Univ. Zaragoza, 525 p.
- RIBA, O., REGUANT, S. and VILLENA, J. 1983: Ensayo de síntesis estratigráfica y evolutiva de la Cuenca Terciaria del Ebro. In: *Libro Jubilar J. M. Ríos. Estudios sobre Geología de España.* II:131-159.
- ROCA, E., 1992: *L'estrucció de la Conca Catalano-balear: paper de la compressió i de la distensió en la seva gènesi.* Ph.D. Thesis, 2 vol., University of Barcelona: 330 p.
- ROCA, E., DESEGUALX, P., FERNÁNDEZ ORTIGOSA, F., ROURE, F. and PINET, B., 1990: Subsidence study and deep structure of the València Trough area. In: B. Pinet and C. Bois (Editors), *The potential of deep seismic profiling for hydrocarbon exploration.* Technip, Paris, pp. 439-443.
- ROCA, E. and GUIMERÀ, J. 1992: The Neogene structure of the eastern Iberian margin: structural constraints on the crustal evolution of the Valencia trough (western Mediterranean). *Tectonophysics*, 203: 203-218.
- SALAS, R., 1987. *El Malm i el Cretaci inferior entre el Massís de Garraf i la Serra d'Espadà.* PhD. Thesis, Univ. Barcelona, 345 p.
- SALAS, R. and CASAS, A. 1993. Mesozoic Extensional Tectonics, Stratigraphy and Crustal Evolution during the Alpine Cicle of the Eastern Iberian Basin. *Tectonophysics*, in press.
- SIMÓN GÓMEZ, J.L. 1980: Estructuras de superposición de plegamientos en el borde NE de la Cadena Ibérica. *Acta Geol. Hispanica*, 15: 137-140.
- SIMÓN GÓMEZ, J.L., 1982: *Compresión y distensión alpinas en la Cadena Ibérica Oriental.* Tesis Doctoral, Univ. Zaragoza, 504 pp. Publ.: Inst. Est. Turolenses, 1984.
- SIMÓN GÓMEZ, J.L., 1989: Late Cenozoic stress field and fracturing in the Iberian Chain and Ebro Basin (Spain). *Jour. Struct. Geol.*, 11(3): 285-294.
- SOLER, J.R., Martínez del Olmo, W., Megías, A.G. and Abegor, J.A., 1983: Rasgos básicos del Neógeno del Mediterráneo español. *Mediterránea*, 1: 71-82.
- SRIVASTA, S.P., SCHOUTEN, H., ROEST, W.R., KLITGORD, K.D., KOVACS, L.C., VERHOEF, J. and MACNAB, R., 1990: Iberian plate kinematics: a jumping plate boundary between Eurasia and Africa. *Nature*, 344: 756-759.
- TAPPONNIER, P., 1977: Evolution tectonique du système alpin en Méditerranée: poinçonnement et écrasement rigide-plastique. *Bull. Soc. Géol. France*, 7ème. sér., 19: 437-460.
- VERGÉS, J., 1993: *Estudi geològic del vessant sud del Pirineu oriental i central. Evolució cinemàtica en 3D.* PhD Thesis, Univ. of Barcelona, Dep. Geologia Dinàmica, Geofísica i Paleontologia, 203 p.